Liver ChREBP Protects Against Fructose-Induced Glycogenic Hepatotoxicity by Regulating L-Type Pyruvate Kinase

Jian-Hui Shi,[1] Jun-Yu Lu,[1] Heng-Yu Chen,[2] Chun-Chun Wei,[1] Xiongfei Xu,[1] Hao Li,[1] Qiufang Bai,[1,2] Fang-Zhen Xia,[3] Sin Man Lam,[4] Hai Zhang,[1] Ya-Nan Shi,[2] Dongmei Cao,[1] Liming Chen,[2] Guanghou Shui,[4] Xia Yang,[5] Yingli Lu,[3] Yu-Xia Chen,[1] and Weiping J. Zhang[1,2]

Diabetes 2020;69:591–602 | https://doi.org/10.2337/db19-0388

Excessive fructose consumption is closely linked to the pathogenesis of metabolic disease. Carbohydrate response element-binding protein (ChREBP) is a transcription factor essential for fructose tolerance in mice. However, the functional significance of liver ChREBP in fructose metabolism remains unclear. Here, we show that liver ChREBP protects mice against fructose-induced hepatotoxicity by regulating liver glycogen metabolism and ATP homeostasis. Liver-specific ablation of ChREBP did not compromise fructose tolerance, but rather caused severe transaminitis and hepatomegaly with massive glycogen overload in mice fed a high-fructose diet, while no obvious inflammation, cell death, or fibrosis was detected in the liver. In addition, liver ATP contents were significantly decreased by ChREBP deficiency in the fed state, which was rendered more pronounced by fructose feeding. Mechanistically, liver contents of glucose-6-phosphate (G6P), an allosteric activator of glycogen synthase, were markedly increased in the absence of liver ChREBP, while fasting-induced glycogen breakdown was not compromised. Furthermore, hepatic overexpression of LPK, a ChREBP target gene in glycolysis, could effectively rescue glycogen overload and ATP reduction, as well as mitigate fructose-induced hepatotoxicity in ChREBP-deficient mice. Taken together, our findings establish a critical role of liver ChREBP in coping with hepatic fructose stress and protecting from hepatotoxicity by regulating LPK.

The increase in fructose consumption has been a particular health concern. Epidemiological studies indicate that excessive and chronic consumption of dietary fructose is strongly linked to the pathogenesis of metabolic syndrome, which is characterized by obesity, insulin resistance, hyperglycemia, dyslipidemia, hypertension, nonalcoholic fatty liver disease, gout, and hyperuricemia (1–5). Fructose and glucose have identical chemical formulas and molecular weights; however, fructose exhibits distinct metabolic features and biological effects in vivo, which may contribute to metabolic diseases (6,7).

Biochemically, the fundamental difference between glucose and fructose metabolism in mammals is their initial phosphorylation (8). Glucose is phosphorylated at the C6-position, and then it is reversibly isomerized into fructose-6-phosphate. Before breakdown into three-carbon units, fructose-6-phosphate has to be further phosphorylated at the C1-position by phosphofructokinase, the most highly regulated enzyme in glycolysis. In contrast, fructose is phosphorylated by ketohexokinase (KHK) at its C1-position to yield fructose-1-phosphate, which can be directly

[1]Department of Pathophysiology, Obesity and Diabetes Research Center, Navy Medical University, Shanghai, China
[2]NHC Key Laboratory of Hormones and Development, Tianjin Key Laboratory of Metabolic Diseases, Tianjin Medical University Chu Hsien-I Memorial Hospital and Tianjin Institute of Endocrinology, Tianjin, China
[3]Institute and Department of Endocrinology and Metabolism, Shanghai Ninth People's Hospital, School of Medicine, Shanghai Jiaotong University, Shanghai, China
[4]State Key Laboratory of Molecular Developmental Biology, Institute of Genetics and Developmental Biology, Chinese Academy of Sciences, Beijing, China
[5]Department of Integrative Biology and Physiology, University of California, Los Angeles, Los Angeles, CA

Corresponding author: Weiping J. Zhang, zbtb20@aliyun.com, or Yu-Xia Chen, yxchen_2013@163.com

Received 22 April 2019 and accepted 15 January 2020

This article contains Supplementary Data online at https://diabetes.diabetesjournals.org/lookup/suppl/doi:10.2337/db19-0388/-/DC1.

J.-H.S., J.-Y.L., and H.-Y.C. contributed equally to this work.

cleaved by aldolase B (AldoB) to dihydroxyacetone phosphate and glyceraldehyde. By bypassing phosphofructokinase, fructolysis is not regulated by product feedback inhibition. Therefore, excess fructose intake leads to uncontrolled consumption of ATP and accumulation of intermediate metabolites, imposing heavy stress to cellular metabolic homeostasis. Intermediate fructose metabolites can enter the gluconeogenesis pathway and are converted into glucose, which occurs in the small intestine and liver, facilitating the disposal of dietary fructose and its metabolites (9). The small intestine absorbs fructose through GLUT5 (10) and can positively regulate its fructose absorption and clearance (9). Excessive dietary fructose overwhelms intestinal absorption and clearance capacity, thereby getting access to the liver and colonic microbiota. Thus, the liver may play an important role in the clearance of excess dietary fructose. However, the mechanism by which the liver copes with such a fructose-induced metabolic stress is not fully understood.

Carbohydrate response element-binding protein (ChREBP) is one of the major transcription factors regulating carbohydrate metabolism and lipogenesis (11–13). Germline deletion of ChREBP leads to liver glycogen accumulation as well as defective hepatic glycolysis and lipogenesis (12). Of note, ChREBP-null mice are intolerant to fructose and become moribund within 1–2 weeks of a diet high in fructose. It was initially speculated that impaired liver fructolysis may contribute to fructose intolerance in ChREBP-null mice. However, conditional gene targeting revealed tissue-specific ablation of ChREBP in the intestine rather than in the liver is the cause of fructose intolerance in mice (14). To date, the functional significance of liver ChREBP in the disposal of excess dietary fructose is still not defined.

In the current study, we demonstrate that liver ChREBP protects mice from fructose-induced hepatotoxicity by regulating hepatic glycogen and ATP homeostasis. Hepatic ChREBP deficiency results in severe liver injury with massive hepatic glycogen accumulation and ATP deficit upon fructose feeding. Mechanistically, glucose-6-phosphate (G6P) contents were markedly elevated in the mutant liver, which allosterically activates glycogen synthesis. Furthermore, hepatic overexpression of LPK could largely rescue the glycogen and ATP phenotypes in mutant mice. Thus, we postulate that liver ChREBP plays a critical role in regulating fructose metabolism and in coping with fructose-induced metabolic stress by controlling the LPK-regulated glycolytic checkpoint.

RESEARCH DESIGN AND METHODS

Generation and Phenotypic Analysis of ChLO Mice

An embryonic stem cell–based strategy was used to generate ChREBP-floxed mice by flanking the eighth exon with LoxP sites. The chimeras were mated with transgenic Flp mice expressing Flp recombinase to delete the neo cassette by Flp-mediated flippase recognition target recombination (15,16). *Chrebp* liver-specific knockout (ChLO) mice were generated by crossing *Chrebp*^{flox} mice with albumin-Cre transgenic mice as previously described (17). PCR primers for genotyping are listed in Supplementary Table 1.

Animal Experiments

All animal experiments were performed on mice that were backcrossed onto C57BL/6J for at least six generations and approved by the Navy Medical University Animal Ethics Committee (Shanghai, China). The mice were fed a normal chow diet (NCD) or high-fructose diet (HFR) (20% protein, 70% fructose, and 10% fat in calories; Shanghai Fanbo Biotechnology Company).

Metabolic Assays

Blood glucose, glucose tolerance test, plasma insulin, plasma and liver triglyceride (TG), cholesterol, and nonesterified fatty acids were measured as previously reported (18). Liver or muscle glycogens were detected with a glycogen assay kit (E2GN-100; BioAssay Systems) in accordance with the manual guidelines included with the kit. For the glucose tolerance test, adult mice were fasted for 6 h prior to i.p. injection of D-glucose (2 g/kg body weight) (19). Plasma aminotransferases were measured in a biochemical analyzer (Mindray BS-220) with the kits provided by the manufacturer (Mindray, Shenzhen, China).

We measured blood glucose using a glucose monitor (One Touch Ultra, Lifescan; Johnson & Johnson, Milpitas, CA); plasma insulin with an ultrasensitive mouse insulin ELISA kit (Mercodia, Uppsala, Sweden); plasma and liver TG, cholesterol, and nonesterified fatty acids by colorimetric assays (Sigma and Wako). We extracted TG and cholesterol from liver with acetone for colorimetric assays. We extracted liver total DNA with a DNA MiNi Kit (QIAamp, 51304) following the operation manual guidelines. We detected liver glycogen with a glycogen assay kit (E2GN-100; BioAssay Systems) following the operation manual guidelines. For the glucose tolerance test, adult mice were fasted for 6 h prior to i.p. injection of D-glucose (2 g/kg body weight).

Periodic Acid Schiff Staining

Sections were oxidized with 0.5% periodic acid for 10 min, stained with Schiff reagent for 30 min at room temperature, followed by restaining with hematoxylin for 30 s Then, the sections were differentiated with 0.1% hydrochloric acid ethanol solution for 1 min and mounted using Permount (DAKO).

Sirius Red Staining

The slides were incubated with a 0.1% Sirius red solution dissolved in aqueous saturated picric acid for 1 h, washed in acidified water (0.5% hydrogen chloride), dehydrated, and mounted with a permanent mounting medium (Sigma).

In Vivo Lipogenesis Assay

We measured hepatic de novo lipogenesis in vivo using [^{3}H]-labeled water as previously described (13). Briefly, mice were i.p. injected with 0.5 mL of 0.15 mol/L NaCl containing 0.2 mCi of [^{3}H]-water/100 g body weight. One

hour later, we excised liver samples (~700 mg per animal), heated them at 90°C for 5 h in a mixture of 1.5 mL of 4 mol/L potassium hydroxide and 1.5 mL of 95% ethanol, and then mixed them with 4 mL of hexane. After centrifugation, we collected the organic phase and dried it for [^{3}H]-sterol assay. The aqueous phase (3 mL) was acidified with 0.75 mL of 10 mol/L H_2SO_4 before mixing with 4 mL hexane and being subjected to centrifugation. Then, we washed the organic phase with 3 mL of distilled water and dried it for the determination of [^{3}H]-labeled fatty acids.

Detection of Liver ATP and Glucose Metabolites

ATP extraction and detection were performed as previously described with some modifications (20). Liver G6P was detected using a G6P assay kit (BioAssay Systems), and uridine diphosphate-glucose (UDPG) was detected by mass spectrometry.

Measurements of Mitochondrial Oxygen Consumption

The primary hepatocytes were isolated by collagenase II perfusion as described elsewhere (21). Mitochondrial respiration was analyzed using the Oxygraph-2k (O2k; OROBOROS Instruments, Innsbruck, Austria) in the presence of various inhibitors.

Microarray Analysis

After feeding 12-week-old mice on a high sucrose diet (60% sucrose) for 1 week, the mice were sacrificed, and liver tissues ($n = 3$ for each group) were collected for use in RNA extraction with RNAiso Reagent (Takara). A microarray analysis was conducted according to the standard protocol of the Shanghai Biotechnology Corporation (Shanghai, China) using Affymetrix GeneChip Mouse Genome 430 2.0 Array, which contains 34,000 annotated genes. Differentially expressed genes with a fold-change >2 and $P < 0.05$ between control and ChLO mice were selected for further analysis. Gene Ontology and Kyoto Encyclopedia of Genes and Genomes enrichment analysis were performed.

mRNA Expression Analysis

mRNA expression was measured by quantitative RT-PCR (qRT-PCR) using the SYBR Green dye-based assay with the *36B4* gene as internal control in every plate. The quantitative PCR primer sequences are listed in the Supplementary Table 2.

Protein Expression Analysis

Whole liver tissue lysates were generated using urea lysis buffer and run on 10% SDS-PAGE gel. Proteins were transferred onto polyvinylidene fluoride membranes (PolyScreen) and incubated in sequential order with the appropriate primary antibody and horseradish peroxidase–conjugated secondary antibodies. This was followed by visualization with enhanced chemiluminescence reagents (Pierce Biotechnology, Rockford, IL). The antibody information and working dilutions are listed in Supplementary Table 3.

Generation of the LPK Adenoviruses

Recombinant adenoviral vectors expressing LPK (Ad-LPK) were purified by CsCl ultracentrifugation and subjected to dialysis against PBS before titration by the standard plaque-forming assay as previously described (18). Ad-GFP or Ad-LPK adenoviruses were delivered via tail-vein injection at a dose of 1×10^{10} plaque-forming unit in a final volume of 200 μL of PBS. Two weeks later, the mice were fed an HFR for another week and then sacrificed.

Statistical Analysis

All numerical data were expressed as mean ± SD. Statistically significant differences among the means of different groups were determined by a two-way ANOVA and defined as $P < 0.05$, except for the mass spectrometry data of glucose metabolites, which were analyzed by the Kruskal-Wallis test.

Data and Resource Availability

The microarray data generated in this study are accessible from the Sequence Read Archive of NCBI with accession number GSE139937. The data sets generated during and/or analyzed during the current study are available from the corresponding author upon reasonable request.

RESULTS

Generation of ChREBP Liver-Specific Knockout Mice

To explore the in vivo function of liver ChREBP, we generated its liver-specific knockout mouse model ChLO using a Cre-LoxP strategy (Fig. 1*A*). To this end, the eighth exon of ChREBP was flanked with the LoxP sites, thereby deleted by albumin promoter–driven Cre in the mutant mice. The targeted allele was distinguished by PCR genotyping using genomic DNA (Fig. 1*B*), and the deletion efficiency and specificity were confirmed at the mRNA and protein levels by qRT-PCR and Western blot analyses, respectively (Fig. 1*C* and *D*). ChLO and control mice were born normally and survived equally into adulthood without any significant gross differences. Expectedly, the liver from the ChLO mice exhibited a remarkable decrease in mRNA expression levels of the ChREBP target genes that are involved in glycolysis and lipogenesis, which include *Pklr*, *Fasn*, *Elovl6*, and *Scd1* compared with the control liver (Fig. 1*E*). These findings are concordant with the results of previous reports (12). As a result, de novo fatty acid synthesis significantly decreased in the mutant liver, whereas sterol synthesis was not affected (Fig. 1*F*). These results indicate the successful generation of a liver-specific ChREBP knockout mouse model and support the critical role of ChREBP in liver glycolysis and lipogenesis.

ChREBP Deficiency Promotes Liver Glycogen Accumulation

When fed on NCD, the ChLO mice exhibited no significant abnormality in body weight or liver weight compared with their control counterparts up to 14 months of

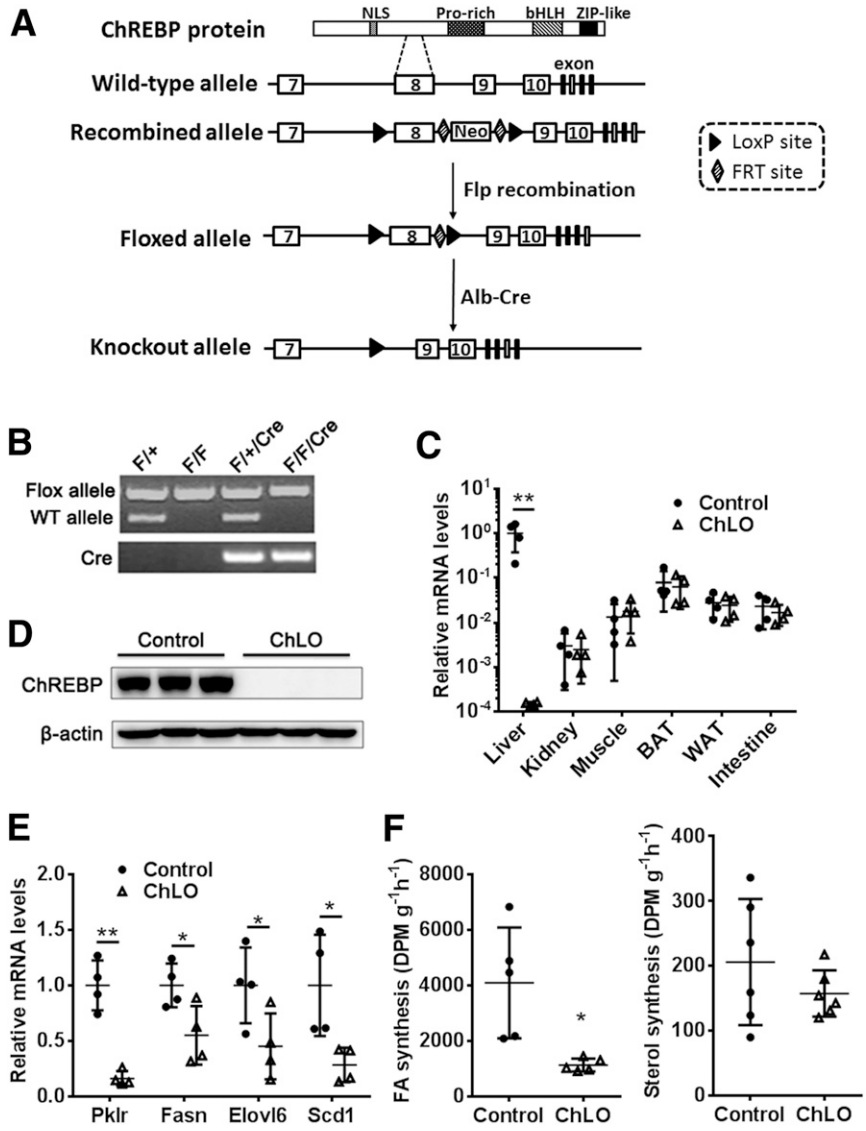

Figure 1—Hepatic de novo lipogenesis (DNL) is impaired in ChLO mice. *A*: Schematic demonstration for the generation of ChREBP liver-specific knockout mice. *B*: Representative demonstration for PCR-based genotyping with tail genomic DNA. *C*: ChREBP deletion efficiency and specificity. ChREBP mRNA levels in liver, intestine, kidney, muscle, brown adipose tissue (BAT), and white adipose tissue (WAT). *D*: Western blot analysis for ChREBP protein expression in the liver. *E*: mRNA levels of glycolytic and lipogenic genes. *F*: Liver DNL was detected with the incorporation of ^{3}H-H_2O in vivo. $^{*}P < 0.05$; $^{**}P < 0.01$. bHLH, basic helix-loop-helix; DPM, disintegrations per minute; FA, fatty acid; NLS, nuclear localization signal; WT, wild type.

age (Supplementary Fig. 1*A* and *B*). The liver of the ChLO mice had a normal appearance and size, and hematoxylin-eosin (H-E) staining of liver sections did not show any obvious morphological abnormality (Supplementary Fig. 1*C*). Plasma transaminase alanine aminotransferase (ALT) and AST levels were normal in both control and ChLO mice, indicating no sign of liver injury (Supplementary Fig. 1*D*). Metabolically, there were no significant alterations in plasma glucose, TG, or insulin levels between the two genotypes, whereas plasma cholesterol levels were slightly but significantly lower in the mutant mice. Oral glucose tolerance test showed a normal glucose disposal in ChLO mice (Supplementary Fig. 2*A*–*D*). Liver TG or total cholesterol contents did not change with ChREBP deletion, while glycogen contents increased by about twofold in the liver and remained constant in skeletal muscle (Supplementary Fig. 2*E* and *F*), which is consistent with a previous report in ChREBP-null mice (12). These results suggest that liver ChREBP plays a critical role in glycogen homeostasis and that mild liver glycogen accumulation alone appears to have no obvious pathological consequences.

Fructose Induces Liver Glycogen Overload and Hepatotoxicity in ChLO Mice

To investigate the role of liver ChREBP in fructose metabolism, we then fed the ChLO and control mice with an HFR, of which 70% of the calories were derived from fructose. Unlike ChREBP-null mice, the ChLO mice did

not show significant differences in body weight or any gross abnormality compared with the control mice within the first 8 weeks of HFR feeding (Fig. 2*A* and Supplementary Fig. 3*A*). Metabolically, both groups of mice had similar plasma glucose levels in the fed or fasting state after 1 week of HFR feeding (Fig. 2*B*). Plasma TG levels did not change in the mutant mice; however, plasma total cholesterol levels significantly decreased compared with the control mice (Fig. 2*C* and Supplementary Fig. 3*B*). These data suggest that liver ChREBP is dispensable for fructose tolerance. These findings are consistent with those of previous reports (14).

Of note, as early as 1 week after the initiation of HFR feeding, the ChLO mice exhibited markedly elevated plasma levels of ALT and AST as well as severe hepatomegaly, with a 61% increase in liver weight–to–body weight ratios relative to the control group (Fig. 2*D* and *E* and Supplementary Fig. 3*C* and *D*). These data suggest fructose might induce hepatotoxicity in the absence of liver ChREBP. H-E staining demonstrated pale staining with obvious architectural changes in the ChLO liver such as hepatic swelling, which was most prominent around the central venous region, whereas the control liver did not show significant abnormalities (Fig. 2*F*). Periodic acid Schiff staining revealed massive glycogen accumulation in fructose-fed ChLO liver compared with the control liver. A biochemical assay confirmed a 4.9-fold glycogen overload in the mutant liver, while muscle glycogen contents were similar between the two genotypes (Fig. 2*G* and Supplementary Fig. 3*E*). Of interest, there was a positive correlation between liver glycogen contents and plasma ALT levels in HFR-fed ChLO mice (Fig. 2*H*). However, levels of liver TG as well as total and free cholesterol contents were significantly lower in the ChLO mice than those of the control group (Fig. 2*I* and Supplementary Fig.

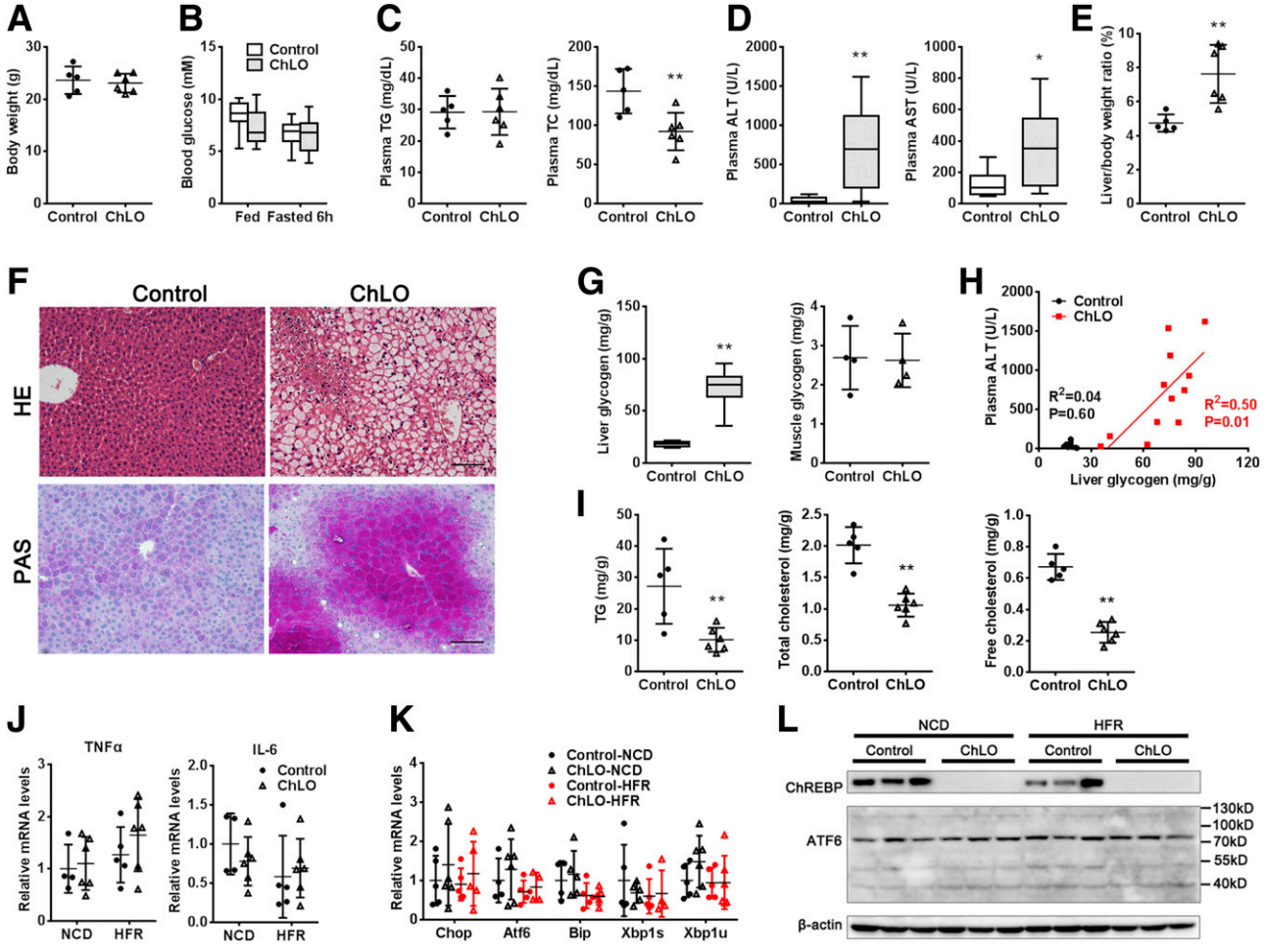

Figure 2—Fructose induces hepatotoxicity and massive liver glycogen accumulation in ChLO mice. *A*: Body weight in control and ChLO groups. *B*: Blood glucose levels in the fed or 6-h-fasted states. *C*: Plasma TG and cholesterol levels in the fed state. *D*: Plasma transaminases levels. *E*: Liver weight/body weight ratios. *F*: Morphological changes demonstrated by H-E staining and PAS staining for glycogen (pink). Scale bar, 100 μm. *G*: Glycogen contents in the liver and muscle in the fed state. *H*: Correlation between liver glycogen contents and plasma ALT levels. *I*: Liver TG and cholesterol contents. *J*: mRNA expression of the inflammatory factors in the liver. *K*: mRNA level of genes involved in ER stress in the liver. *L*: Western blot analysis for ATF6 expression and activation. $n = 5–12$. $^*P < 0.05$; $^{**}P < 0.01$. IL, interleukin; PAS, periodic acid Schiff; TC, total cholesterol.

3*F*). These data imply that liver glycogen overload could be a cause of the fructose-induced hepatotoxicity.

To further characterize the pathology of fructose-induced hepatotoxicity in the absence of ChREBP, we measured distinct forms of cell death. TUNEL staining revealed sparse apoptotic cells in the HFR-fed liver, and no significant differences in apoptotic cells as well as the activation of caspase 3 were observed between the two genotypes (Supplementary Fig. 4*A*–*C*). In addition, after 1 or 8 weeks of HFR feeding, the ChLO and control mice had comparable plasma levels of lactate dehydrogenase and glutamate dehydrogenase (Supplementary Fig. 4*D* and *E*), which are indicators of hepatocyte necrosis (22,23). Western blot analysis of necroptotic biomarkers revealed no significant change in the expression or phosphorylation of RIP, RIP3, and MLKL in the liver of ChLO mice challenged with high fructose for 1–8 weeks compared with the control group (Supplementary Fig. 4*F*).

We further assessed inflammation and endoplasmic reticulum (ER) stress, which are frequently involved in liver injury (24,25). qRT-PCR analysis revealed that 1 or 8 weeks of HFR feeding did not significantly change the mRNA levels of proinflammatory factors interleukin 6 and tumor necrosis factor-α in either the control or mutant liver compared with those fed on regular chow diet, and there were no significant differences between the two genotypes when the mice were fed with NCD or HFR (Fig. 2*J* and Supplementary Fig. 5*A*). Moreover, the activation of nuclear factor-κB and c-Jun N-terminal kinase, which are two key proteins involved in proinflammatory signal pathways, was not significantly altered in HFR-fed mutant liver compared with the control group (Supplementary Fig. 5*B*). Additionally, the

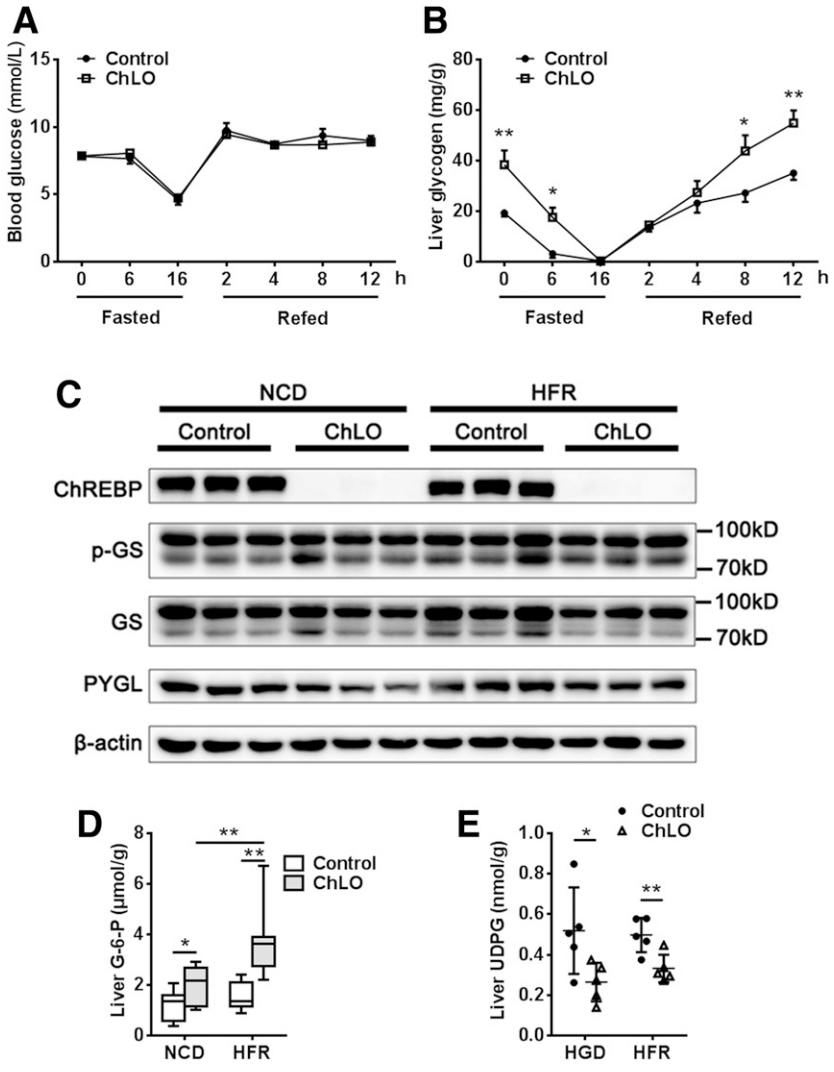

Figure 3—Liver glycogen synthesis is enhanced in the absence of ChREBP. *A*: Plasma glucose levels after fasting and refeeding with chow diet. *B*: Liver glycogen contents after fasting and refeeding with chow diet. Four to six male mice per group. *C*: Western blot analysis for GS and glycogen phosphorylase in liver from chow or HFR-fed mice. p-GS, phosphorylated GS. *D*: Liver G6P from chow or HFR-fed mice in the fed state. *E*: Liver UDPG from high-glucose diet (HGD) or HFR-fed mice in the fed state. $^{*}P < 0.05$; $^{**}P < 0.01$.

expression of putative markers for ER stress, Chop, Bip, and XBP1s as well as ATF6 protein levels and activation, were similar between the control and ChLO mice fed on HFR (Fig. 2*K* and *L*). Sirius red staining showed relatively little collagen deposition in the livers of either control or mutant mice after 8 weeks of HFR feeding (Supplementary Fig. 5*C*). Transforming growth factor-β1 and α-SMA protein expression levels were similar in the two genotypes (Supplementary Fig. 5*D*). Taken together, these findings suggest that the fructose-induced hepatotoxicity in ChLO mice is associated with glycogen overload, without overt cell death, inflammation, ER stress, or fibrosis, per se, which resembles glycogenic hepatopathy (26).

ChREBP Regulates Liver Glycogen Metabolism

To understand the mechanism by which liver ChREBP deficiency causes glycogen accumulation, we observed the dynamics of plasma glucose levels and liver glycogen contents in the fasting/refeeding experiments. The chow-fed ChLO and control mice were fasted up to 16 h, followed by refeeding normal chow up to 12 h, during which similar changes in plasma glucose levels were observed between the two groups (Fig. 3*A*). After 6 h of fasting, liver glycogen was almost undetectable in the control mice but remained at a remarkable level in ChLO mice, roughly close to that in nonfasting control mice (Fig. 3*B*). After 16 h of fasting, both groups of mice showed depletion of liver glycogen, suggesting its breakdown, and glucose output might be not affected by the loss of ChREBP. During the first 4 h of chow refeeding, glycogen accumulation in the liver of ChLO mice was similar to that in the control mice. However, after 8 h of refeeding, liver glycogen contents significantly increased in the mutant mice compared with the control mice, which implied enhanced glycogen synthesis.

Next, we analyzed the expression and activity of glycogen synthase (GS), a key enzyme involved in glycogen synthesis. GS is activated by dephosphorylation through inactivation of GS kinase-3 with insulin and by the allosteric stimulator G6P (27). Western blot analyses revealed that liver GS expression and phosphorylation levels were comparable between the ChLO and control mice (Fig. 3*C*). Interestingly, liver contents of G6P increased by 70% in chow-fed ChLO mice compared with the control mice (Fig. 3*D*). Moreover, liver G6P contents increased even more dramatically when mutant mice were fed with HFR, which coincides with its more prominent phenotype of liver glycogen accumulation. Consistently, the increase of liver G6P has been reported in ChREBP-null mice (12,28). In contrast, the levels of UDPG, a direct and active substrate for glycogen synthesis, significantly decreased in the mutant liver (Fig. 3*E*), which might be a result of enhanced glycogen synthesis. Therefore, accumulation of the liver glycogen in the mutant mice is likely the result of allosteric effects of increased G6P that occurs with feeding rather than changes in GS or glycogen phosphorylase abundance or their activity/phosphorylation status.

ChREBP Regulates Hepatic ATP Homeostasis

Considering the critical role of ChREBP in glycolysis and the energy-consuming nature of both fructose phosphorylation and glycogen synthesis, we examined whether the fructose-induced hepatotoxicity in ChLO mice was associated with compromised ATP homeostasis. The chow-fed control mice showed an increase in liver ATP contents in the fed state compared with the fasted state, while the change disappeared in HFR-fed control mice (Fig. 4*A*). In the fasted state, the ChLO mice had comparable liver ATP contents with the control whether they were fed the chow diet or HFR prior to fasting. In contrast, under fed conditions, chow-fed mutant mice showed a mild but significant reduction in liver ATP levels relative to control mice. More importantly, 1 week of HFR feeding caused a significant decrease in liver ATP contents in both genotypes compared with their chow-fed counterparts. As a result, the HFR-fed mutant mice showed an ~40% reduction in liver ATP levels compared with the chow-fed control mice in the fed state. Furthermore, the fasting/refeeding test

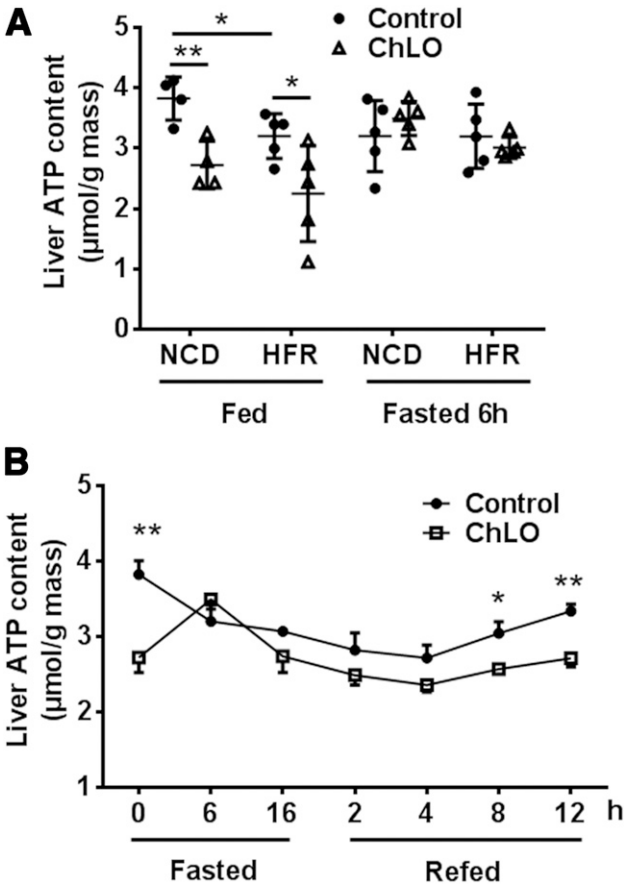

Figure 4—ChREBP regulates hepatic ATP homeostasis under the feeding condition. Eight-week-old male ChLO and control mice were fed with HFR or NCD as control for 1 week. *A*: Liver ATP contents under the fed or 6-h-fasting condition. *B*: Dynamics of liver ATP contents in the control and ChLO mice during fasting and NCD refeeding. $n = 5$. *$P < 0.05$; **$P < 0.01$.

revealed a decrease in liver ATP levels in ChLO mice compared with the control after 12 h of HFR refeeding (Fig. 4*B*). These results imply that compromised ATP homeostasis might be a contributing factor to fructose-induced hepatotoxicity in the absence of ChREBP.

ChREBP is Required for the Expression and Fructose-Induced Activation of LPK in the Liver

To understand the molecular mechanism by which ChREBP protects organisms from fructose-induced hepatotoxicity, we first characterized the change of gene expression profiles in response to lack of liver ChREBP. The liver tissues of mice fed a high-sucrose diet (60% sucrose in calories) were subjected to microarray analysis. A total of 34,000 genes were annotated, which included 90 upregulated genes and 112 downregulated genes. The top 32 differentially expressed genes are shown in the heat map, which include Pklr and Khk. Gene Ontology and Kyoto Encyclopedia of Genes and Genomes enrichment analyses revealed that the most enriched pathways were associated with metabolism, including TG metabolic process, acylglycerol metabolic process, single-organism carbohydrate catabolic process, and neutral lipid metabolic process (Supplementary Fig. 6), which coincides with the observed phenotypic changes and the major effects of ChREBP in known metabolic processes.

Then we characterized the expression patterns of genes involved in fructose metabolism. As expected, fructose feeding resulted in a robust increase in Pklr mRNA and its protein LPK levels in the control liver compared with that in chow-fed mice (Fig. 5*A* and *B*). A slight or mild increase in the mRNA levels of ChREBP-β, Khk, Tkfc, and Fbp1 was observed. HFR did not significantly change the protein levels of KHK, AldoB, FBP1, or G6pc in the control liver compared with chow diet. Deletion of ChREBP led to a marked reduction in liver *Pklr* mRNA and protein levels in chow- or HFR-fed mice, and to a lesser extent, of *Khk*, *Fbp1*, and *G6pc*, whereas AldoB protein levels were slightly or hardly affected despite its mild reduction in mRNA levels. These results suggest that liver *Pklr* is a fructose-responsive gene highly regulated by ChREBP and might act as a checkpoint in fructose metabolism, thereby controlling glycolysis and ATP production.

To determine whether ChREBP ablation causes a hepatic mitochondria defect per se, thereby compromising ATP production, we first analyzed mitochondrial contents. PCR analysis showed similar amount of mtDNA in the ChLO and control liver from mice fed on either chow or HFR, including Cox2 and mtND1 (Supplementary Fig. 7). Furthermore, western blot analysis revealed that the components of the respiratory chain complex were comparably expressed at the protein levels in both chow- and HFR-fed groups. Moreover, in vitro oxygen consumption analysis demonstrated comparable mitochondrial function in isolated primary hepatocytes from both genotypes. Together, these findings suggest that the ATP decline in the ChLO liver is unlikely due to the dysfunction of hepatic mitochondria per se.

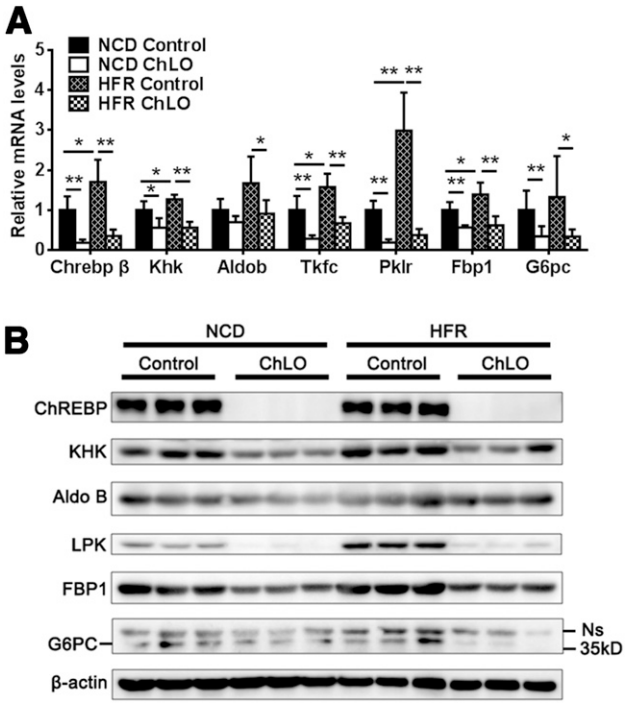

Figure 5—ChREBP is required for LPK expression and responsiveness to fructose stimulation. Adult ChLO and control mice were fed HFR or NCD diet as control for 1 week starting at 8 weeks of age. Four to six mice per group. *A*: The expression of genes involved in fructose metabolism was analyzed at the mRNA level. *B*: The expression of genes involved in fructose metabolism was analyzed at the protein level. $^{*}P < 0.05$; $^{**}P < 0.01$. Ns, nonspecific band.

LPK Overexpression Rescues Fructose-Induced Liver Injury in ChLO Mice

Given that LPK is highly responsive to fructose and critical for glycolysis, we reasoned that its defect might be an important factor in fructose-induced hepatotoxicity in the ChLO mice. To test this hypothesis, we overexpressed LPK in the control and ChLO liver by intravenous injection of adenoviruses expressing LPK (Ad-LPK) or GFP (Ad-GFP) as control. Two weeks after adenovirus administration, the mice were fed on the HFR for another week before sacrifice. Administration of Ad-LPK resulted in overexpression of LPK in the liver rather than extrahepatic tissues including skeletal muscle, heart, white adipose tissue, and kidney (Fig. 6*A* and Supplementary Fig. 8). After 1 week of HFR feeding, Ad-GFP–treated ChLO mice showed apparent hepatomegaly and liver injury, with elevated plasma ALT levels compared with the control genotype. LPK overexpression could largely or even completely restore liver weight–to–body weight ratio in ChLO mice compared with the GFP control (Fig. 6*B* and *C*). Accordingly, their morphological abnormalities (e.g., pale staining and hepatocyte swelling), as well as plasma transaminase levels, were also almost completely restored in the ChLO mice upon LPK overexpression (Fig. 6*B* and *D*). Moreover, liver glycogen accumulation, ATP levels, and G6P contents were largely corrected in Ad-LPK–treated ChLO liver under fed status (Fig. 6*E* and *F*). However, LPK

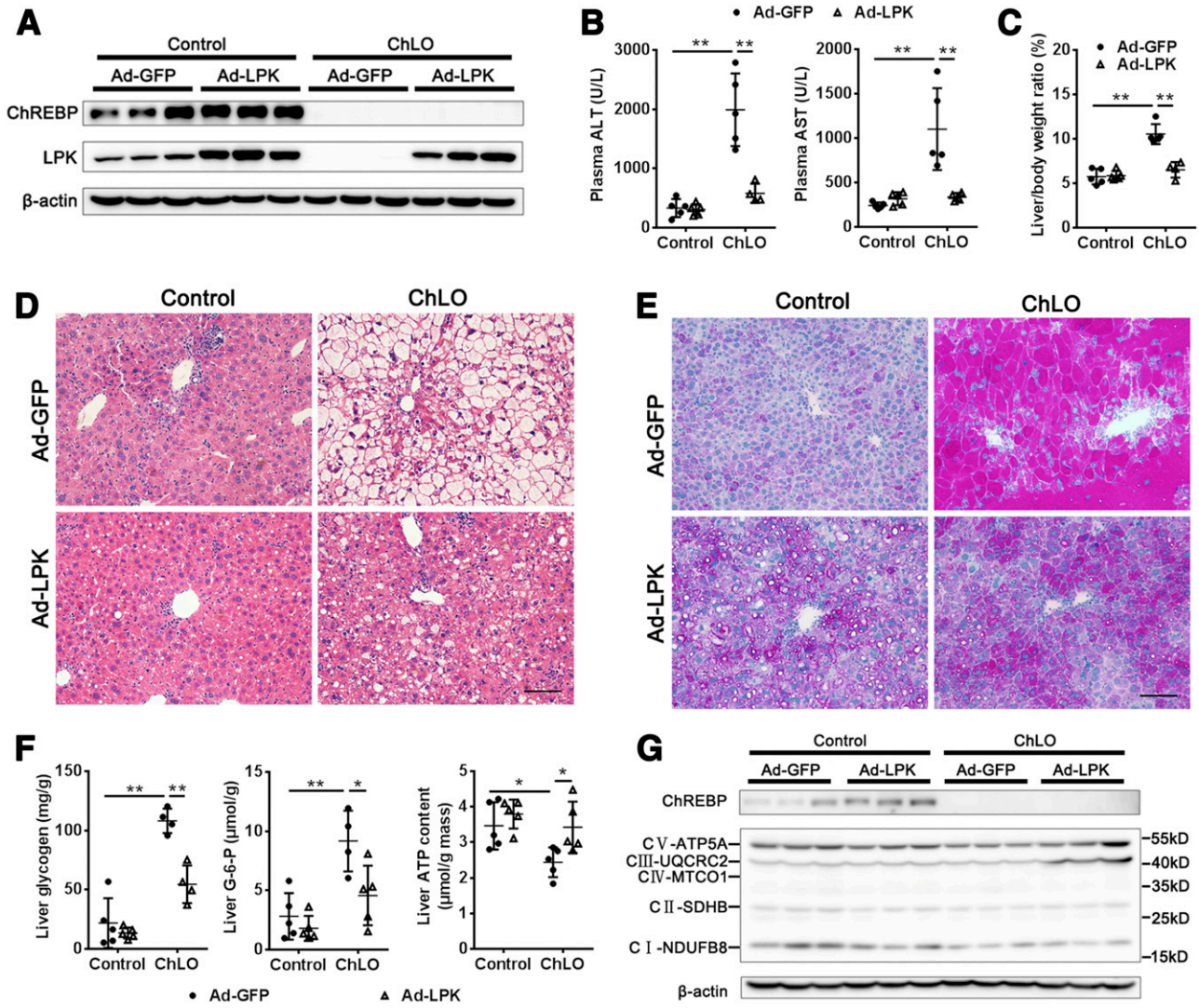

Figure 6—LPK overexpression restores ATP homeostasis and rescues fructose-induced liver injury in ChREBP-deficient mice. Two-month-old control and ChLO mice were i.v. injected with adenoviruses Ad-LPK or Ad-GFP as control. Two weeks later, the mice were fed with HFR for 1 week before sacrifice. *A*: Western blot analysis for protein levels of ChREBP and LPK in the livers. *B*: Plasma transaminases levels. *C*: Liver weight–to–body weight ratio. *D*: H-E staining of liver sections. Scale bar, 100 μm. *E*: Periodic acid Schiff staining of liver sections. Scale bar, 100 μm. *F*: Liver contents of glycogen, ATP, and G6P in the control and ChLO mice. *G*: Western blot analysis of liver mitochondrial respiratory complex. $n = 5$. $^*P < 0.05$; $^{**}P < 0.01$. U, units.

overexpression did not significantly affect the components of the mitochondrial respiratory chain complex (Fig. 6*G*). These data suggest that inhibited LPK expression largely, or at least partly, accounts for fructose-induced hepatotoxicity with glycogen overload and ATP decline in the absence of liver ChREBP (Fig. 7).

DISCUSSION

Liver glycogen accumulation has been described in the global as well as liver-specific ChREBP knockout mice (12,14,29,30); however, its biochemical mechanism and pathological significance was not well appreciated. Although the phenotype was linked to impaired glycolysis or downregulation of *G6pc*, the causal relationship has not been validated (12,14,28). The current study establishes the role of ChREBP-regulated LPK in hepatic glycogen and ATP homeostasis in the fed state. First, we performed the fasting/refeeding test to demonstrate that this glycogen phenotype is primarily caused by enhanced glycogen synthesis in the fed state, while fasting-induced glycogen breakdown is not significantly impaired in the absence of ChREBP. Second, consistent with previous reports in global ChREBP knockouts (12,28), we provided direct biochemical evidence that liver contents of G6P, the allosteric activator of GS (31), were markedly elevated in the mutant mice, despite constant levels of expression and phosphorylation of GS. As a result, UDPG, the active substrate for glycogen synthesis, significantly decreased in the mutant liver, excluding the possibility of substrate-driven glycogen overproduction. Of note, G6pc expression was mildly reduced in

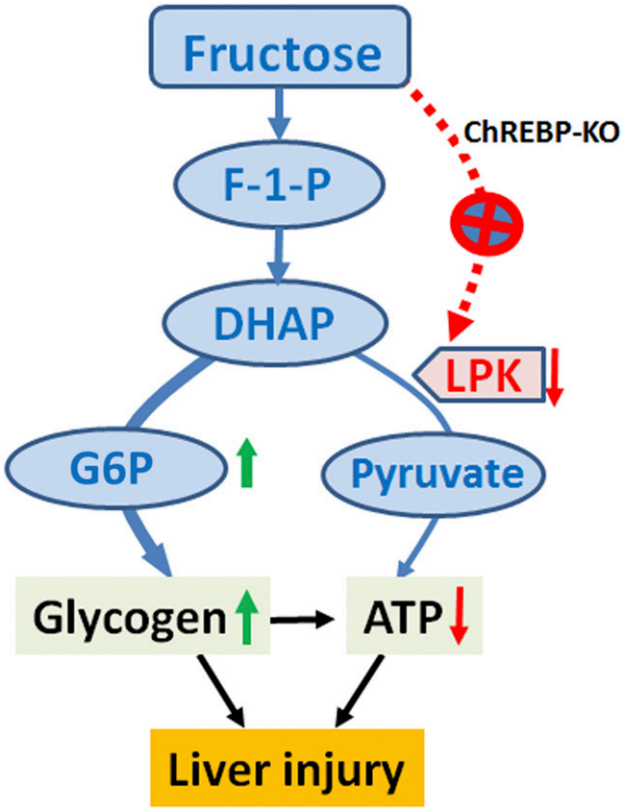

Figure 7—Schematic model for fructose-induced glycogenic hepatotoxicity in the absence of liver ChREBP. In the absence of ChREBP, the LPK is not activated and loses its responsiveness to fructose stimulation, leading to a defect of LPK-controlled glycolysis and ATP production. As a consequence, hepatic G6P is accumulated, which robustly stimulates glycogen synthesis at the expense of ATP consumption. This causes massive hepatic glycogen accumulation coupled with ATP deficit, thus contributing to the pathogenesis of fructose-induced glycogenic hepatotoxicity. DHAP, dihydroxyacetone phosphate; F-1-P, fructose-1-phosphate.

the ChLO liver, which encodes glucose-6-phosphase catalyzing the dephosphorylation of G6P. As a target gene of ChREBP, G6pc plays a critical role in liver glycogen homeostasis and glucose output (28,32,33). Homozygous liver-specific G6pc knockout mice exhibit severe liver glycogen overload with G6P elevation (33); however, these changes were not described in the heterozygotes. Therefore, whether G6pc contributes to G6P elevation and resultant glycogen accumulation in the ChLO mice will be an intriguing subject to explore in the future. Third, liver ATP contents are diminished by ChREBP deficiency in the fed state rather than in the fasted state, which is most likely caused by the impaired glycolysis and resultant ATP production due to LPK downregulation. In addition, the increase in ATP consumption in excessive fructose phosphorylation and glycogen synthesis could be another contributing factor. This is supported the observation that the ATP reduction is more dramatic with fructose challenge and lags behind the increase of glycogen contents in mutant liver during refeeding after fasting. Lastly, LPK overexpression can effectively reduce liver glycogen and G6P accumulation, and restore ATP contents in the mutant mice, suggesting that LPK is a checkpoint for the regulation of glycogen synthesis and ATP homeostasis by ChREBP. As a canonical target of ChREBP (34), LPK is a key enzyme of glycolysis. We postulate that ChREBP-regulated LPK not only directly promotes glycolytic flux and subsequent ATP production, but also prevents excessive glycogen synthesis and ATP consumption due to allosteric overactivation of GS by G6P (Supplementary Fig. 9). Therefore, both diminished production and excessive consumption of ATP in glycogen synthesis contribute to the decline in liver ATP contents in chow-fed mutant mice in the fed state, whereas KHK-mediated uncontrolled fructose phosphorylation is another driving force for excessive ATP consumption in HFR-fed mice. Burgess et al. (35) demonstrates an increase in pyruvate dehydrogenase complex activity in the liver from global ChREBP knockout mice, which causes impaired fatty acid oxidation and stimulated lactate and pyruvate oxidation. Whether pyruvate dehydrogenase complex activity is altered and contributes to the ATP reduction in the ChLO liver are under further investigation. So far, our findings suggest that ChREBP-regulated LPK at least partly contributes to hepatic energy homeostasis. Our previous work shows that the zinc finger protein ZBTB20 regulates de novo lipogenesis in the liver through ChREBP (18). Interestingly, excessive liver glycogen accumulation is also present in liver-specific Zbtb20 knockout mice (17,18). Whether ZBTB20 also contributes to hepatic ATP homeostasis requires further investigation.

This study also established the critical role of liver ChREBP in protecting from fructose-induced hepatotoxicity. Unlike the global ChREBP knockout, the ChLO mice are fructose tolerant. However, the mutant mice exhibit severe liver injury when fed an HFR, which suggest that ChREBP is indispensable for the liver to dispose of excessive dietary fructose. Of note, the fructose-induced hepatotoxicity in the absence of liver ChREBP is associated with hepatic glycogen overload and ATP deficit, with no signs of inflammation, ER stress, steatosis, or fibrosis, which is mostly consistent with the described features of glycogenic hepatopathy (26,33). Moreover, their liver glycogen accumulation and ATP decrease are much more severe than chow-fed counterparts, and there is a positive correlation between liver glycogen overload and plasma ATL levels. Given that ATP deficiency can cause the disorder of water and electrolytes metabolism, it is most likely that glycogen overload coupled with ATP insufficiency contributed to the pathogenesis of fructose-induced glycogenic liver injury in the absence of ChREBP. Whether ChREBP mutation causes human glycogenic hepatopathy requires further investigation.

Although most of the genes involved in hepatic fructose metabolism are regulated by ChREBP, our finding strongly points to LPK as a critical checkpoint controlling fructose metabolism and tolerance in the liver. First, liver expression of LPK shows a robust responsiveness to fructose feeding in normal control mice, while other ChREBP targets

(e.g., Khk, AldoB, Fbp1, and G6pc) respond poorly to fructose stress in terms of mRNA and protein expression levels. The mechanism underlying the differential responsiveness of the ChREBP targets to fructose stimulation needs to be investigated in the future. Second, LPK mRNA and protein expression are dramatically decreased in the liver by the deletion of ChREBP, while those of Khk, Fbp1, G6pc, and AldoB are slightly or hardly affected. Third, overexpression of LPK in the liver can efficiently rescue the phenotypes of hepatomegaly, liver glycogen overload, and ATP deficit, as well as the elevated plasma transaminases induced by fructose in ChREBP mutant mice. Lastly, hepatic mitochondria, per se, are not affected by the loss of ChREBP in our study. ChLO mice appear normal in terms of the number and respiratory chain complex components. Of note, LPK regulates mitochondrial functions (36), which presumably results from a defect in the availability of LPK-produced pyruvate to the trichloroacetic acid cycle. Therefore, we conclude that LPK-regulated glycolysis is a critical checkpoint for fructose metabolism. Under normal circumstances, LPK is substantially activated by fructose through ChREBP, thereby enhancing glycolysis and ATP production, which helps in coping with the metabolic stress involving the uncontrolled generation of fructose-1-phosphate at the expense of ATP and to maintain the homeostasis of hepatic glycogen and bioenergy. In the absence of ChREBP, LPK is not activated and loses its responsiveness to fructose stimulation in the liver. Consequently, liver glycolysis and ATP production are profoundly inhibited, while glycogen synthesis is greatly enhanced. Both fructose phosphorylation and glycogen synthesis largely contribute to excessive ATP consumption, as well as exacerbate hepatic ATP insufficiency in the setting of diminished production in the mutant liver. Taken together, our findings strongly suggest that ChREBP plays a critical role in liver fructose metabolism, protecting against fructose-induced glycogenic hepatopathy at least partially through LPK.

Our finding that liver ChREBP has a protective role in coping with excess fructose is discordant to those of others (14,37). Jois et al. (37) generated a liver-specific ChREBPa knockout mice with the deletion of exon 1a, while the alternative promoter and expression cassette of ChREBP-β was intact (38). They demonstrated that deletion of hepatic ChREBP caused insulin resistance but did not change liver glycogen contents or the expression of ChREBP target genes in liver glycolysis and lipogenesis. Kim et al. used a liver-specific knockout model with the deletion of exons 9–15 (30), and they demonstrated an approximately twofold increase in liver glycogen contents and a mild increase in plasma ALT levels in HFR-fed mutant mice, without significant morphological abnormality in the liver (14). The most likely explanation for the marked difference in fructose-induced liver response is the genetic background of the mouse. We used ChLO mice on a mixture of C57BL/6J and J129S3 genetic backgrounds, which have been backcrossed to C57BL/6J at least for six generations. Kim et al. (14) used mice with a mixed background of C3H/HeJ and C57BL/6J. C3H/HeJ mice are more sensitive to fructose-induced obesity and insulin resistance than C57BL/6J (39). It is interesting to note that the control mice used by Kim et al. are responsive to fructose stimulation in terms of the liver G6pc gene rather than LPK (14), which is the opposite in our control mice. Nevertheless, the mechanism and biological significance of differential responsiveness of the ChREBP target genes to fructose requires further investigation.

Fructose-induced glycogenic hepatopathy in our ChLO mice is also quite different from that observed by Zhang et al. (29) in ChREBP global knockout mice. They reported severe steatohepatitis in ChREBP-null mice fed on a HFR, which is accompanied by a threefold increase in liver glycogen contents, unfolded protein reaction, enhanced cholesterol biosynthesis, and hepatocyte apoptosis. In contrast, except for the common glycogen overload in the liver, our ChLO mice did not exhibit inflammation, steatosis, unfolded protein reaction, or hepatocyte apoptosis. Moreover, liver cholesterol synthesis was not significantly affected in the HFR-fed ChLO liver, while their total and free cholesterol contents decreased compared with the control, which also agrees with the findings of Kim et al. (14). One possibility for the observed difference is mouse model. Zhang et al. (29) utilized ChREBP global knockout mice with a pure C57BL/6J background (12), which should have a defect in intestinal fructose absorption (14). Therefore, fructose-induced liver inflammation in this mouse model could potentially be secondary to progressive sepsis and associated endotoxemia resulting from a combination of intestinal dysfunction, reduced food intake, and weight loss. In addition, endotoxemia can enhance cholesterol synthesis in rodent models, which might explain the liver cholesterol phenotype in the global knockout mice.

Collectively, our findings provide novel insights into the physiological role of liver ChREBP in glycolysis and fructose metabolism, which helps in unraveling the biochemical basis of fructose-induced glycogenic liver injury and in developing novel therapeutic approaches to the disease.

Acknowledgments. The authors are thankful to Xianhua Ma (Navy Medical University) for technical assistance in histological examination and Dr. Yan Wang and Rui Yang (Navy Medical University) for their help in the adenoviral preparation and injection.

Funding. This work was supported by grants from National Natural Science Foundation of China (91857203 and 31730042), National Key RD Program of China (2019YFA0802500 and 2018YFA0800603), and Natural Science Foundation of Shanghai (18ZR1449400).

Duality of Interest. No potential conflicts of interest relevant to this article were reported.

Author Contributions. W.J.Z. and J.-H.S. contributed to study concept and design. J.-H.S., Y.-X.C., H.-Y.C., C.-C.W., J.-Y.L., Q.B., H.L., S.M.L., F.-Z.X., D.C., and H.Z. contributed to data acquisition. J.-H.S., Y.-X.C., H.Z., G.S., Y.-N.S., L.C., X.Y., Y.L., and W.J.Z. analyzed data, and W.J.Z., Y.-X.C., and J.-H.S. wrote the manuscript. X.Y. edited the manuscript. W.J.Z., Y.-X.C., and X.X. obtained funding, and W.J.Z. contributed to study supervision. W.J.Z. is the guarantor of this work and, as such, had full access to all the data in the study and takes responsibility for the integrity of the data and the accuracy of the data analysis.

References

1. Lim JS, Mietus-Snyder M, Valente A, Schwarz JM, Lustig RH. The role of fructose in the pathogenesis of NAFLD and the metabolic syndrome. Nat Rev Gastroenterol Hepatol 2010;7:251–264
2. Stanhope KL. Role of fructose-containing sugars in the epidemics of obesity and metabolic syndrome. Annu Rev Med 2012;63:329–343
3. Douard V, Ferraris RP. The role of fructose transporters in diseases linked to excessive fructose intake. J Physiol 2013;591:401–414
4. Jegatheesan P, De Bandt JP. Fructose and NAFLD: the multifaceted aspects of fructose metabolism. Nutrients 2017;9:E230
5. Caliceti C, Calabria D, Roda A, Cicero AFG. Fructose intake, serum uric acid, and cardiometabolic disorders: a critical review. Nutrients 2017;9:E395
6. Patel C, Douard V, Yu S, Gao N, Ferraris RP. Transport, metabolism, and endosomal trafficking-dependent regulation of intestinal fructose absorption. FASEB J 2015;29:4046–4058
7. Samuel VT. Fructose induced lipogenesis: from sugar to fat to insulin resistance. Trends Endocrinol Metab 2011;22:60–65
8. Hannou SA, Haslam DE, McKeown NM, Herman MA. Fructose metabolism and metabolic disease. J Clin Invest 2018;128:545–555
9. Jang C, Hui S, Lu W, et al. The small intestine converts dietary fructose into glucose and organic acids. Cell Metab 2018;27:351–361.e3
10. Barone S, Fussell SL, Singh AK, et al. Slc2a5 (Glut5) is essential for the absorption of fructose in the intestine and generation of fructose-induced hypertension. J Biol Chem 2009;284:5056–5066
11. Yamashita H, Takenoshita M, Sakurai M, et al. A glucose-responsive transcription factor that regulates carbohydrate metabolism in the liver. Proc Natl Acad Sci U S A 2001;98:9116–9121
12. Iizuka K, Bruick RK, Liang G, Horton JD, Uyeda K. Deficiency of carbohydrate response element-binding protein (ChREBP) reduces lipogenesis as well as glycolysis. Proc Natl Acad Sci U S A 2004;101:7281–7286
13. Dentin R, Pégorier JP, Benhamed F, et al. Hepatic glucokinase is required for the synergistic action of ChREBP and SREBP-1c on glycolytic and lipogenic gene expression. J Biol Chem 2004;279:20314–20326
14. Kim M, Astapova II, Flier SN, et al. Intestinal, but not hepatic, ChREBP is required for fructose tolerance. JCI Insight 2017;2:96703
15. Rodríguez CI, Buchholz F, Galloway J, et al. High-efficiency deleter mice show that FLPe is an alternative to Cre-loxP. Nat Genet 2000;25:139–140
16. Li L, Gao L, Wang K, et al. Knockin of Cre gene at Ins2 locus reveals no Cre activity in mouse hypothalamic neurons. Sci Rep 2016;6:20438
17. Xie Z, Zhang H, Tsai W, et al. Zinc finger protein ZBTB20 is a key repressor of alpha-fetoprotein gene transcription in liver. Proc Natl Acad Sci U S A 2008;105:10859–10864
18. Liu G, Zhou L, Zhang H, et al. Regulation of hepatic lipogenesis by the zinc finger protein Zbtb20. Nat Commun 2017;8:14824
19. Sutherland AP, Zhang H, Zhang Y, et al. Zinc finger protein Zbtb20 is essential for postnatal survival and glucose homeostasis. Mol Cell Biol 2009;29:2804–2815
20. Kim JS, Qian T, Lemasters JJ. Mitochondrial permeability transition in the switch from necrotic to apoptotic cell death in ischemic rat hepatocytes. Gastroenterology 2003;124:494–503
21. Zhang Y, Xie Z, Zhou L, et al. The zinc finger protein ZBTB20 regulates transcription of fructose-1,6-bisphosphatase 1 and β cell function in mice. Gastroenterology 2012;142:1571–1580.e6
22. Van Waes L, Lieber CS. Glutamate dehydrogenase: a reliable marker of liver cell necrosis in the alcoholic. BMJ 1977;2:1508–1510
23. Chan FK, Moriwaki K, De Rosa MJ. Detection of necrosis by release of lactate dehydrogenase activity. Methods Mol Biol 2013;979:65–70
24. Kaplowitz N, Than TA, Shinohara M, Ji C. Endoplasmic reticulum stress and liver injury. Semin Liver Dis 2007;27:367–377
25. Han J, Kaufman RJ. The role of ER stress in lipid metabolism and lipotoxicity. J Lipid Res 2016;57:1329–1338
26. Torbenson M, Chen YY, Brunt E, et al. Glycogenic hepatopathy: an underrecognized hepatic complication of diabetes mellitus. Am J Surg Pathol 2006;30:508–513
27. Bouskila M, Hunter RW, Ibrahim AF, et al. Allosteric regulation of glycogen synthase controls glycogen synthesis in muscle. Cell Metab 2010;12:456–466
28. Kim MS, Krawczyk SA, Doridot L, et al. ChREBP regulates fructose-induced glucose production independently of insulin signaling. J Clin Invest 2016;126:4372–4386
29. Zhang D, Tong X, VanDommelen K, et al. Lipogenic transcription factor ChREBP mediates fructose-induced metabolic adaptations to prevent hepatotoxicity. J Clin Invest 2017;127:2855–2867
30. Linden AG, Li S, Choi HY, et al. Interplay between ChREBP and SREBP-1c coordinates postprandial glycolysis and lipogenesis in livers of mice. J Lipid Res 2018;59:475–487
31. Villar-Palasí C, Guinovart JJ. The role of glucose 6-phosphate in the control of glycogen synthase. FASEB J 1997;11:544–558
32. Fisher FM, Kim M, Doridot L, et al. A critical role for ChREBP-mediated FGF21 secretion in hepatic fructose metabolism. Mol Metab 2016;6:14–21
33. Mutel E, Abdul-Wahed A, Ramamonjisoa N, et al. Targeted deletion of liver glucose-6 phosphatase mimics glycogen storage disease type 1a including development of multiple adenomas. J Hepatol 2011;54:529–537
34. Hasegawa J, Osatomi K, Wu RF, Uyeda K. A novel factor binding to the glucose response elements of liver pyruvate kinase and fatty acid synthase genes. J Biol Chem 1999;274:1100–1107
35. Burgess SC, Iizuka K, Jeoung NH, et al. Carbohydrate-response element-binding protein deletion alters substrate utilization producing an energy-deficient liver. J Biol Chem 2008;283:1670–1678
36. Chella Krishnan K, Kurt Z, Barrere-Cain R, et al. Integration of multi-omics data from mouse diversity panel highlights mitochondrial dysfunction in non-alcoholic fatty liver disease. Cell Syst 2018;6:103–115.e7
37. Jois T, Chen W, Howard V, et al. Deletion of hepatic carbohydrate response element binding protein (ChREBP) impairs glucose homeostasis and hepatic insulin sensitivity in mice. Mol Metab 2017;6:1381–1394
38. Herman MA, Peroni OD, Villoria J, et al. A novel ChREBP isoform in adipose tissue regulates systemic glucose metabolism. Nature 2012;484:333–338
39. Nagata R, Nishio Y, Sekine O, et al. Single nucleotide polymorphism (-468 Gly to A) at the promoter region of SREBP-1c associates with genetic defect of fructose-induced hepatic lipogenesis [corrected] [published correction appears in J Biol Chem 2004;279:37210]. J Biol Chem 2004;279:29031–29042